NACA

RESEARCH MEMORANDUM

SURVEY OF AVAILABLE INFORMATION ON INTERNAL FLOW LOSSES THROUGH AXIAL TURBOMACHINES

By Chung-Hua Wu

Lewis Flight Propulsion Laboratory
Cleveland, Ohio

NATIONAL ADVISORY COMMITTEE
FOR AERONAUTICS

WASHINGTON
January 26, 1951

NATIONAL ADVISORY COMMITTEE FOR AERONAUTICS

RESEARCH MEMORANDUM

SURVEY OF AVAILABLE INFORMATION ON INTERNAL FLOW LOSSES THROUGH AXIAL TURBOMACHINES

By Chung-Hua Wu

SUMMARY

Due to the scattered nature of existing information on the losses involved in the internal flow of gases through axial compressors and turbines, a brief survey of the available information on such losses is made. The present state of knowledge and the direction of future research toward the reduction of these losses are indicated.

INTRODUCTION

A part of the current losses in the gas flow through a turbomachine could be attributed to the imperfection in the present design method, such as the lack of a blade-design method based on the three-dimensional main flow, the lack of a quantitative knowledge of the radial motion of the viscous boundary layer along the blades, and so forth. The rest of the loss is due to such unavoidable factors as the blade-wake loss, the radial and axial clearances between rotating and stationary members, the unsteady nature of flow between successive blade rows, and so forth. Avoidance of losses of the first kind and reduction of losses of the second kind require a much more thorough understanding of the unsteady, three-dimensional compressible flow of the viscous gas inside these machines than is now available.

This paper, which was prepared at the NACA Lewis laboratory, presents a brief summary of the scattered information pertinent to the evaluation of the aerodynamic losses in axial turbomachines, which may indicate the present state of knowledge and the direction of future research toward the reduction of these losses.

The losses that are not due to the viscosity of the gas or that can be treated with a nonviscous fluid will first be discussed. The losses that are closely associated with the viscous-flow phenomena are then discussed.

SYMBOLS

The following symbols are used in this report:

$b=r_t-r_h$	blade span or height of blade
C	blade chord
C_a	axial chord
C_D	drag coefficient
C_L	lift coefficient
c	tip clearance
D	drag force
e	induced incidence at midspan
g_e	leakage flow loss
H	δ^*/δ^{**}
L	lift force
l_e	end loss
K_r	ratio of kinetic energy in secondary flow to mean work output of rotor
M	Mach number
N	number of blades
n	normal distance
P'	loss in total pressure
R'	resistance of airfoil in cascade
r	radial distance from axis of rotation
S,t	spacing or pitch
T	kinetic energy in secondary flow per unit blade span

U	rotor velocity
V	absolute velocity of gas
W	velocity of gas relative to blade
α	gas angle measured with respect to machine axis
β	blade angle measured with respect to machine axis
Γ	circulation
γ	ratio of specific heats
δ^*	displacement thickness
δ^{**}	momentum thickness
η	efficiency
ρ	density
σ	solidity ratio
ζ	cascade stagger angle measured with respect to axis

Subscripts:

a	axial component
h	hub
i	induced
k	trailing edge
p	profile
R	rotor
S	stator
t	tip
u	tangential component

0	stagnation value
1	entrance
2	exit or where boundary layers from different airfoils in cascade emerge
1_∞	far ahead of blade
2_∞	far behind blade

THREE-DIMENSIONAL FLOW OF MAIN MOTION

Axial turbomachines are usually designed at present on the basis of two-dimensional flow; that is, the flow of gas is assumed to take place along cylindrical surfaces and the effect of radial motion is neglected. Theoretical investigation (reference 1) indicates that the periodic change in the circumferential velocity of gas through successive blade rows is accompanied by a periodic outward and inward radial motion of the gas. The neglect of the curvature of streamline caused by the oscillatory radial flow and the radial shift of mass flow causes an error in the determination of the radial distribution of gas velocities and, consequently, the blade is set at a wrong angle of attack, thus operating at a less efficient point at the design condition and resulting in a shorter range of off-design operation. The error becomes greater with the use of a velocity diagram other than the free-vortex type, tapered inner and outer walls, high axial velocity of gas flow, low inlet hub-to-tip radius ratio, and high aspect ratio. The loss involved due to this factor can be avoided if a method of through-flow calculation and blade design based on three-dimensional flow of the main stream is developed. The method of blade design should be general enough to take, as its inlet flow, whatever rotational flow profile exists at the exit of the preceding blade row, which may be caused by a number of reasons discussed later. The solution of the three-dimensional distribution of the main stream is also important in obtaining quantitative information about the three-dimensional behavior of the boundary layer over the blade surface.

Induced Loss Due to Design Variation of Circulation along Blade Span

In inlet and exit guide vanes, which invariably deflect the gas with quite different angles at different radii, the design circulation

around the blade section varies along the blade span. In rotors and stators between them, the circulation may also be nonuniform along the span in order to have some desirable radial variation of flow conditions other than that given by the free-vortex tangential velocity distribution. As a result of circulation variation along the span, vortices are continuously shed from the trailing edge of the blade into the main stream and carried downstream. The kinetic energy associated with the secondary motion of gas behind the blade is usually taken as the induced loss. It is not known how much of this kinetic energy could be recovered in a following blade row; hence the whole amount of kinetic energy may be used for comparing the induced loss inherent to various types of velocity diagram.

For lightly loaded blades, the secondary flow can be conveniently studied by the classical lifting-line theory of Prandtl. For blades with large camber, some modification of the theory or a different approach is necessary.

Considering compressor blades with small camber, and expressing the circulation variation along the span as a Fourier cosine series

$$\Gamma(r) = \sum_{n=0}^{\infty} a_n \cos n\pi \frac{r-r_h}{r_t-r_h} \tag{1}$$

Tsien (reference 2) gives the following formula for the downwash velocity due to trailing vortices:

$$W_{u,i} = \frac{n}{4(r_t-r_h)} \sum_{n=1}^{\infty} n\, a_n \coth \frac{n\pi S \cos \zeta}{2(r_t-r_h)} \cos n\pi \frac{r-r_h}{r_t-r_h} \tag{2}$$

For a linear variation of lift along the span and constant chord, the following expression for the total induced drag of one blade is also obtained:

$$D_i = \frac{\rho}{2} W^2 C(r_t-r_h) \frac{(C_{L,h}-C_{L,t})^2}{\pi^3} \frac{C}{r_t-r_h} \left[1.0518 + \sum_{n=1,3,5} \frac{\coth \frac{n\pi S \cos \zeta}{2(r_t-r_h)} - 1}{n^3} \right] \tag{3}$$

It is seen from equation (3) that the loss due to this source would be quite small. Carter (reference 3) applies this formula to a typical compressor of hub-to-tip radius ratio of 0.7 and obtains a value of $C_{D,i}$ of only 0.003, which indicates that compressor designs based on velocity diagrams other than free-vortex type would not give excessive induced losses.

Induced Loss Due to Nonuniform Inlet Flow

The inlet flow to all blade rows may be quite nonuniform due to the use of a nonvortex velocity diagram in design, or it may become nonuniform in later stages of a multistage machine due to the discrepancy between the actual flow and that used in the design of blades, and the effect of boundary layer along the hub and casing walls. A general linearized theory of a wing subjected to a nonuniform inlet flow was given by von Kármán and Tsien in reference 4, in which general expressions of induced velocity and induced drag are presented. This theory can be directly applied to compressor blades of small deflection.

In an unpublished report, Squire and Winter recently extended von Kármán and Tsien's theory to the flow with large deflection in a straight cascade of airfoils. The method is based on a linear combination of a perturbation flow and the two-dimensional flow about the blade section. The change of vorticity is then obtained by an integration along the two-dimensional streamlines. In a pipe bend, Hawthorne (reference 5) found that the secondary flow is not spiral but oscillatory. It will be interesting to see whether similar phenomena occur in turbine and compressor blade rows.

UNSTEADY FLOW

The state of gas leaving a blade row is not uniform circumferentially, which gives a time varying inlet flow to the following blade row moving relatively to the preceding one. This periodically varying inlet flow leads to a periodically varying circulation over the blade and, consequently, vortices of periodically varying strength are shed from the trailing edge of the blade (fig. 1). For blades with small deflections, the secondary motion may be investigated by applying the lifting-line theory. For the case of a simple sinusoidal variation of circulation in two-dimensional flow, Keller (reference 6) obtained the following expression for the kinetic energy in the secondary flow per unit blade span:

$$T = \frac{1}{16} \pi \rho (\Delta\Gamma)^2 \, (1 + 2R) \qquad (5)$$

where $\Delta\Gamma$ is the variation in circulation per unit span and $(1+2R)$ represents the grid effect with

$$R = \frac{e^{-2\pi h/l} \cos 2\pi \frac{a}{l} - e^{-4\pi h/l}}{1-2e^{-2\pi h/l} \cos 2\pi \frac{a}{l} + e^{-4\pi h/l}} \tag{6}$$

where

$$h = S_R \cos \beta_2 \tag{7}$$

$$l = S_S \frac{W_2}{U} \tag{8}$$

$$a = S_R \sin \beta_2 + \frac{W_2}{U} (S_R - S_S) \tag{9}$$

(See fig. 1.) The following expression for the ratio of this loss to the rotor blade output in the case of a single-stage turbine of small loading and with no tangential velocity leaving the rotor was also obtained:

$$K_r = \frac{\pi}{4} (1+2R) \frac{N_S}{N_R} \left(\frac{\Delta\Gamma}{2\Gamma}\right)^2 \frac{\Delta V_u}{V_a} \tag{10}$$

where ΔV_u is the change in tangential velocity across the rotor blade and R is determined by equation (6) with

$$\frac{a}{l} = 1 - \frac{N_S}{N_R} \cos^2 \beta_2 \tag{11}$$

and

$$\frac{h}{l} = \frac{1}{2} \frac{N_S}{N_R} \sin 2\beta_2 \tag{12}$$

The theoretical questions still remaining are: (1) What is the relation between circulation variation and the variation of approach velocity? and (2) How much of this kinetic energy in the secondary motion could be recovered in the next row of blades, if there is one?

One effective way to reduce this loss is to place the blades as far apart as practical to allow the gas to uniformize in the circumferential direction. One typical variation for a reaction turbine is shown in figure 2, taken from unpublished data of the Wright Aeronautical Corporation.

BLADE-PROFILE LOSS

Resistance of Airfoil in Cascade in Two-Dimensional Subsonic Flow

In comparison with the case of an isolated airfoil, the theoretical calculation of the drag or resistance of an airfoil in cascade is complicated by the interaction of the boundary layers associated with individual airfoils in the cascade. Based on a slight non-homogeneity of the flow in the section of the aerodynamic wake where the boundary layers of their individual airfoils merge (plane 2 - 2 in fig. 3), Loitsianskii (reference 7) derived the following formula for the resistance (in the axial direction) of airfoils in cascade:

$$R' = P't = \left[\rho_m W_{2\infty}^2 + \frac{1}{4}(H_2-1)\,\rho_{2\infty}\left(W_{2\infty}^2 - W_{1\infty}^2\right)\right]\frac{\delta_2^{**}}{\cos \alpha_{2\infty}} \tag{13}$$

where

$$\rho_m = \frac{1}{2}(\rho_{1\infty} + \rho_{2\infty}) \tag{14}$$

and

$$\delta_2^{**} = \int_{y_0'}^{y_0'+t'} \frac{\rho W}{\rho_2 W_2}\left(1 - \frac{W}{W_2}\right) dy_2' \tag{15}$$

In equation (15) the primes indicate the value in the direction normal to W_2.

Equation (13) reduces to

$$R' = \rho W_{2\infty}^2 \frac{\delta_2^{**}}{\cos \alpha_2} \tag{16}$$

in the case of incompressible flow past a cascade of airfoils; and

$$R' = \rho_\infty V_\infty^2 \, \delta_\infty^{**} \tag{17}$$

in the case of incompressible flow past an isolated airfoil, as given by Squire and Young (reference 8).

Equation (13) gives the pressure loss or resistance of an airfoil in cascade, for compressible flow, in terms of known quantities at stations far ahead and far behind the blade and the quantities H_2 and δ_2^{**} at station 2, the position of which remains unknown because up to now there is no reliable theory of the turbulent wake. Loitsianskii generalized the method of Squire and Young to relate them to the boundary-layer condition at the trailing edge of the blade k-k obtaining

$$\left(\frac{W_k}{W_{2\infty}}\right)^{\frac{H_2}{2}} \frac{(\gamma-1)\, M_{2\infty}^2 - (H_2-1)}{\frac{1}{2}(\gamma-1)\, M_{2\infty}^2 + 1} = \frac{\theta_k}{\delta_k^{**}} \left(\frac{W_{2\infty}}{W_{k\infty}}\right)^{1+\frac{H_k}{2}} \tag{18}$$

$$\delta_2^{**} = \left[\frac{1 + \frac{\gamma-1}{2} M_{2\infty}^2}{1 + (\gamma-1)\, M_{2\infty}^2 - H_2}\right] \frac{\rho_k W_k}{\rho_{2\infty} W_{2\infty}} \, \theta_k \tag{19}$$

where θ is a thickness of energy loss defined by

$$\theta = \int_{-\infty,\delta}^{\infty,\delta} \frac{\rho W_S}{\bar{\rho}\bar{W}_S} \left(1 - \frac{T_0}{\bar{T}_0}\right) dn \tag{20}$$

In equation (19), the bar over the quantity denotes its value at the outer limit of the boundary layer. Now, δ_k^{**} and θ_k are either measurable or computable by any method of the theory of the boundary layer and in terms of the velocity, density, and temperature at the outer limit of the boundary layer near the trailing edge of the airfoil and at a station far behind the cascade. After H_2 and δ_2^{**} are found from equations (18) and (19), R' is obtained from equation (13). If the ordinary drag defined in the direction of W_m is desired, it is equal to $R' \cos \alpha_m$. (See fig. 2.) These results are believed to be very basic in nature and should be very useful in the investigation of two-dimensional profile resistance.

Variation of Blade-Profile Loss with Reynolds Number, Incidence, Mach Number, Solidity, Trailing-Edge Thickness, and Trailing-Edge Taper

Some typical experimentally determined variations of blade-profile loss with Reynolds number and so forth are shown in figures 4 to 10. Figure 4 shows the variation of profile loss of turbine blades with Reynolds number based on gas outlet velocity obtained by Ainley (reference 9). This indicates a critical Reynolds number of about 10^5 for blades operating in a turbine where the mean turbulence is higher than that in cascade. For compressor blades, Howell (reference 10) gives the critical Reynolds number as 1 to 3×10^5 based on inlet-air velocity. Figures 5 and 6 show the variation of profile loss with incidence of a typical compressor and a turbine blade, respectively. It is seen that the loss is more sensitive to the incidence angle on the positive side in both cases and the range of operation is much narrower and greatly reduced by high Mach number for compressor blades (fig. 5) but not as much for turbine blades (fig. 7).

The effect of blade solidity on loss is conveniently expressed in figure 8 by Howell (reference 11) through a factor λ, which is equal to $(6-\sigma)/5$. The lift and drag coefficients are all defined on the exit velocity.

A method of determining minimum required cascade solidity for a given turning is given by Goldstein and Mager (reference 12), which is based on empirical data of boundary-layer behavior over isolated airfoils. The effects of maximum surface velocity, Reynolds number, and blade thickness are considered.

The effect of blade-surface finish on efficiency is discussed by Sörensen in reference 13. As long as the boundary layer is thicker than the greatest protuberance of the roughness of the surface, the roughness cannot affect the flow and the blade surface can be considered as aerodynamically smooth. The required fineness of finish therefore increases with higher Reynolds number of flow. A uniform definition of roughness and some experimental determination of the variation of the friction loss with the amount of protuberance of surface roughness in excess of the boundary-layer thickness will be useful to the turbomachine designers.

Based on the assumption that the effect of blade-edge thickness is simply causing a dead-air region immediately downstream equal to

the blade trailing-edge thickness, the increase in blade loss due to this low-velocity region is estimated by taking $k = 0$ for a width equal to the trailing-edge thickness in the following loss formula given by Reeman and Simonis (in an unpublished paper) for the case of an incompressible fluid and assuming that the fluid leaves the blade space with a uniform static pressure and direction:

$$\frac{P'}{P_{1\infty}} = \frac{1 + \left(\int k ds\right)^2 - 2\int k^2 ds + \tan^2\alpha_2 \left[1 - \left(\frac{\int k^2 ds}{\int k ds}\right)^2\right]}{1 + \tan^2\alpha_2 + 2\left[\left(\int k ds\right)^2 - \int k^2 ds\right]} \tag{21}$$

where $k = V/V_{max} = f(s)$ and is estimated by using the seventh-power law in the boundary-layer region.

The results of Reeman and Simonis indicate that the blade outlet angle has little effect on trailing-edge-thickness loss except for outlet angles greater than 60° and that there is little to be gained in reducing trailing-edge thickness below 2 or 3 percent of the spacing. Some of these theoretical values are compared with the experimental values in figure 9.

Some typical variations of wake profile with different trailing-edge thickness and taper and the accompanying blade efficiency are shown in figure 10.

Radial Flow of Boundary Layer in Turbomachine

In applying two-dimensional theoretical and experimental results to a blade section in a turbomachine, care must be taken that the effect of radial displacement of flow in the boundary layer along the blade surface is taken into account. Betz first reported that the fluid in a boundary layer flows outward along the blade in the case of propeller and blower blades (reference 14) and, as a consequence, the inner section could be loaded considerably higher before separation occurs and the outer section correspondingly less than those in a stationary two-dimensional cascade. This phenomenon is further experimentally confirmed by Weske (reference 15). The outward radial motion of the boundary-layer fluid in these cases can be explained by the fact that the rotative speed of the fluid particles in the boundary layer is greater than that in the main fluid and requires for equilibrium a radial pressure gradient greater than that imposed on them

by the main stream. In the case of the turbine rotor, the circumferential velocity of the main stream is usually greater than the rotor speed for a certain distance downstream of the leading edge of the blade and, consequently, the larger inward radial pressure gradient in the main stream tends to force the boundary-layer fluid radially inward. Over the rest of the blades, the reverse is true, and the boundary layer moves radially outward.

In a stationary blade, the radial pressure gradient in the main stream always causes the boundary-layer fluid to move inward toward the axis of the machine.

In reference 16, Weske discusses qualitatively the secondary-motion boundary layer in stationary or rotating-blade grids with or without circulatory motion at the outlet section. He also analyzes the radial displacement of boundary layer in a free-vortex main stream by the use of the Euler equation (reference 17).

The importance of this problem cannot be overemphasized. More quantitative theoretical and experimental data are urgently needed for the design of high-performance turbomachines.

FLOW OF BOUNDARY LAYER ALONG INNER AND OUTER ANNULUS WALLS

In reference 18, Burgers discussed the effect of the circumferential velocity of the main flow and the wall rotation on the viscous boundary layer along the inner and outer annulus walls of turbomachines. That analysis shows that: (1) The existence of tangential velocity of the main stream has the effect of a retarding force when the radius of the wall increases but also helps the transition of the boundary layer into a turbulent one; and (2) the rotation of the inner wall has the effect of driving the fluid toward the section of larger diameter and hence reduces the chance of separation when the radius of the wall increases.

The viscous boundary layer on the inner and outer annulus walls directly gives the so-called annulus loss. Eckert, Pflüger, and Weinig (reference 19) account for this loss by simply proportioning it to the profile drag according to the respective surface area. Howell (reference 10) accounts for this loss by the use of an annulus drag coefficient equal to 0.02 S/b.

This direct frictional loss due to the boundary-layer flow along the annulus walls amounted to only 1/10 to 2/10 of the total losses in turbomachines. The greater effect on losses is through the secondary flow in the main stream, as described in the next section.

SECONDARY-FLOW LOSSES DUE TO FLOW DEFLECTION AND BOUNDARY-LAYER FLOW ALONG ANNULUS WALLS

Due to the curvature in the flow through the blades, there is a pressure gradient in the gas stream from the convex surface of one blade toward the concave surface of the next blade. Owing to the boundary layer along inner and outer walls, the velocity of the gas near the boundary layer is lower and, consequently, the pressure gradient from the convex surface to the concave surface is correspondingly lower. Hence, the gas pressure at the concave surface near the walls is less than that at the midspan of the blade, whereas the gas pressure at the convex surface near the walls is higher than that at the midspan of the blade. Consequently, a secondary flow such as shown in figure 11 is set up. Because they are unstable, the vortices roll up into two trailing vortices. This phenomenon can also be explained through the sudden drop of circulation in the annulus boundary layer, thereby shedding trailing vortices. For relatively thin boundary layers, these two rolled-up vortices are close to the walls. Its essential effect is to give high losses near the end walls (fig. 12) and reduce the effective incidence to the blade and, consequently, the lift and the deflection (fig. 13). Based on lifting-line theory, simple approximate formulas were obtained by Carter and Cohen (reference 3) for the induced incidence at the midspan and the induced drag coefficient:

$$e = \frac{1}{4} \sigma C_L \left(1 - \frac{b'}{b}\right) \tag{22}$$

$$C_{D,i} = \frac{1}{4} \sigma C_L^2 \left(1 - \frac{b'}{b}\right) \frac{b'}{b} \tag{23}$$

where b' is the distance between the two vortices to be determined experimentally.

Hausmann (reference 20) investigated induced flow in a cascade and obtained a more general expression for the value of downwash velocity. His numerical result shows that induced deflection angle rapidly increases with boundary-layer displacement thickness and decreases slightly with the number of blades.

TIP-CLEARANCE LOSS

In the clearance space between the blade and the casing wall, gas flows from the pressure surface of the blade to the suction surface. Consequently, the streamline on the pressure side has an additional velocity component toward the clearance space, whereas the streamline on the suction side has an additional velocity away from the clearance space (fig. 14), giving a surface of discontinuity of velocity at the trailing edge. If the tip clearance lies within the boundary layer, the effect caused by this leakage flow is felt through a modification of the boundary-layer thickness or the value b' in equations (22) and (23). The separation of the tip-leakage loss from the induced flow associated with wall boundary layer is difficult. The tip-leakage loss is further complicated by the relative motion of the wall, which strengthens tip-leakage flow in the case of the compressor, whereas it opposes the tip-leakage flow in the case of the turbine (figs. 15 and 16).

In spite of these complications, the theoretical effect of tip leakage alone is useful to help analyze the problem. As early as 1925, Betz (reference 21) obtained the following expression for the minimum induced drag due to tip leakage (based on classical airfoil theory of small deflection):

$$C_{D,i} = \frac{L^2}{\frac{1}{2}\rho W_m^2 b^2} k_2 \tag{24}$$

where

$$k_2 = \frac{K\left(\tanh \frac{\pi c}{S \cos \alpha_2}\right)}{8K\left(1/\cosh \frac{\pi c}{S \cos \alpha_2}\right)} \tag{25}$$

and

$$K(\lambda) = \int_0^1 \frac{dx}{\sqrt{1-x^2}\sqrt{1-\lambda^2 x^2}} \tag{26}$$

An approximate expression of k_2 is given by Meldahl (reference 22) as

$$k_2 \approx \frac{1}{4}\left(\frac{c}{S \cos \alpha_2} + \frac{\log_e 2}{\pi}\right) \tag{27}$$

Meldahl's tests on single-stage reaction turbines indicate an approximately linear variation of efficiency with tip clearance and suggest the percentage flow loss g_e and work loss l_e in the following formula for efficiency as a linear function of the ratio of tip clearance to blade width:

$$\eta = \eta_p - \frac{l_e}{b/C_a + g_e} \tag{28}$$

In the blade tested,

$$l_e = 0.1011 + 4.667\ c/C_a \tag{29}$$

$$g_e = -0.0422 + 2.790\ c/C_a \tag{30}$$

For c/C_a varying between 0.04 and 0.08, the loss attributed to the clearance is about three-quarters of the total induced loss.

An investigation by Ruden (reference 23) on a single-stage compressor also indicates an approximately linear variation of efficiency with tip clearance.

AN APPROXIMATE OVER-ALL PICTURE OF INTERNAL FLOW LOSSES

Considering the blade-profile loss the same as in the two-dimensional cascade investigation, an annulus friction loss as that given by Howell, and the remaining losses as the secondary-flow loss, a general picture of the variation of losses in a typical compressor and turbine is shown in figures 17 and 18, respectively. Although the division between the profile loss and the secondary-flow loss in the actual machine is inconclusive, it is apparent that the future improvement in efficiency and performance will be gained through the improvement of blade-design technique, so that the blade will operate at the most desirable incidence angle, and the reduction in secondary losses from various sources.

Lewis Flight Propulsion Laboratory,
National Advisory Committee for Aeronautics,
Cleveland, Ohio.

REFERENCES

1. Wu, Chung-Hua, and Wolfenstein, Lincoln: Application of Radial-Equilibrium Condition to Axial-Flow Compressor and Turbine Design. NACA Rep. 955, 1950. (Formerly NACA TN 1795.)

2. Tsien, Hsue-Shen: Loss in Compressor or Turbine Due to Twisted Blades. C.I.E. Jour., 1947, pp. 40-53.

3. Carter, A. D. S.: Three-dimensional-flow Theories for Axial Compressor and Turbines. War Emergency Issue No. 41, pub. by Inst. Mech. Eng. (London). (Reprinted in U.S. by ASME, April 1949, pp. 255-268.)

4. von Kármán, Theodore, and Tsien, Hsue-Shen: Lifting-Line Theory for a Wing in Non-Uniform Flow. Quart. Appl. Math., vol. III, no. 1, April 1945, pp. 1-11.

5. Hawthorne, William R.: Secondary Circulation in Fluid Flow. Gas Turbine Lab., M.I.T., May 1950.

6. Keller, C.: Kinetic Energy Losses behind Blade Grids as a Result of Periodic Variation in the Circulation. Rep. Inst. Aero., Tech. Hochschule (Zurich), 1934, pp. 167-187. (Available as R.T.P. Trans. No. 1883, British M.A.P.)

7. Loitsianskii, L. G.: Resistance of a Cascade of Airfoils in a Gas Flow with Subsonic Velocities. NACA TM 1303, 1950.

8. Squire, H. B., and Young, A. D.: The Calculation of the Profile Drag of Aerofoils. R. & M. No. 1838, British A.R.C., Nov. 1937.

9. Ainley, D. G.: Performance of Axial-flow Turbines. War Emergency Issue No. 41 pub. by Inst. Mech. Eng. (London). (Reprinted in U.S. by ASME, April 1949, pp. 230-244.)

10. Howell, A. R.: The Present Basis of Axial Flow Compressor Design. Part I. Cascade Theory and Performance. R. & M. No. 2095, British A.R.C., June 1942.

11. Howell, A.R.: The Aerodynamics of the Gas Turbine. R.A.S. Jour., vol. LXX, 1948, pp. 329-348; discussion, pp. 348-356.

12. Goldstein, Arthur W., and Mager, Artur: Attainable Circulation about Airfoils in Cascade. NACA Rep. 953, 1950. (Formerly NACA TN 1941.)

13. Sörensen, E.: Wandrauhigkeitseinfluss bei Strömungsmaschinen. Forschung auf dem Gebiete des Ingenieurwesens, Bd. 8, Heft 1, Jan./Febr. 1937, S. 25-29.

14. Betz, A.: Axial Superchargers. NACA TM 1073, 1944.

15. Weske, J. R.: Investigation of Blade Characteristics. Trans. A.S.M.E., vol. 66, no. 5, July 1944, pp. 413-418; discussion, pp. 419-420.

16. Weske, John R.: Fluid Dynamic Aspects of Axial-Flow Compressors and Turbines. Jour. Aero. Sci., vol. 14, no. 11, Nov. 1947, pp. 651-656.

17. Weske, J. R.: Secondary Flows in Rotating Blade Passages at High Reynolds Numbers. Proc. Seventh Int. Cong. for Appl. Mech., vol. 2, pt. 1, 1948, pp. 155-163.

18. Burgers, J. M.: Some Considerations on the Development of Boundary Layers in the Case of Flows Having a Rotational Component. Nederl, Akad. van Wetenschappen, vol. XLIV, Nos. 1-5, 1941, pp. 12-25.

19. Eckert, B., Pflüger, F., and Weinig, F.: The Influence of the Diameter Ratio on the Characteristics Diagram of the Axial Compressor. NACA TM 1125, 1948.

20. Hausmann, George F.: The Theoretical Induced Deflection Angle in Cascades Having Wall Boundary Layers. Jour. Aero. Sci., vol. 15, no. 11, Nov. 1948, pp. 686-690.

21. Betz, A.: Über die Vorgänge an den Schaufelenden von Kaplan-Turbinen. Ein Wissenschaftlischer Überblick Vortrage auf der Hydraliketagung (Göttingen), AM 5 und 6, Juni 1925, S. 161-179.

22. Meldahl, A.: End Losses of Turbine Blades. Jour. Am. Soc. Naval Eng., vol. 54, no. 3, Aug. 1942, pp. 454-466.

23. Ruden, P.: Investigation of Single Stage Axial Fans. NACA TM 1062, 1944.

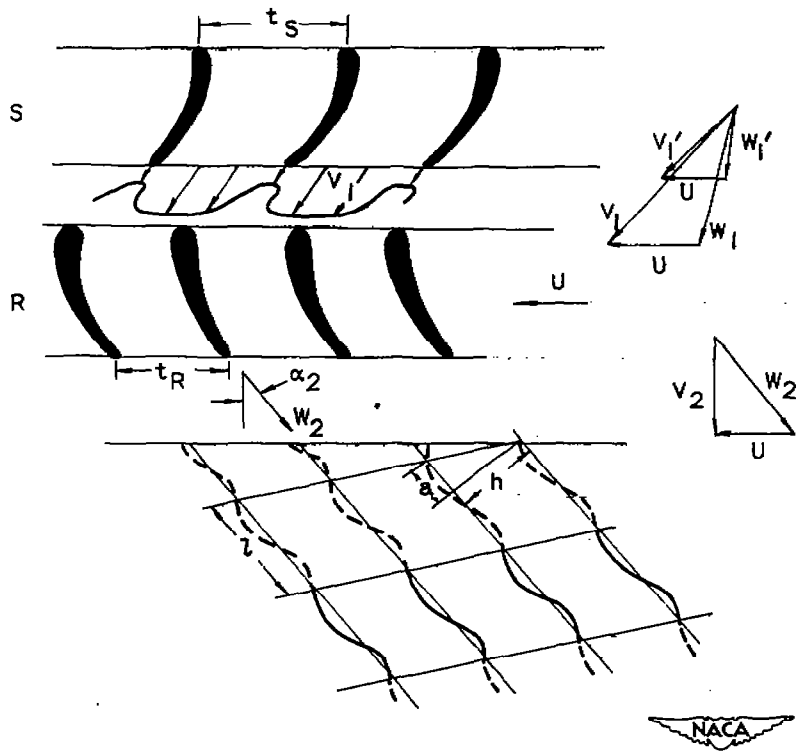

Figure 1. - Loss due to unsteady flow.

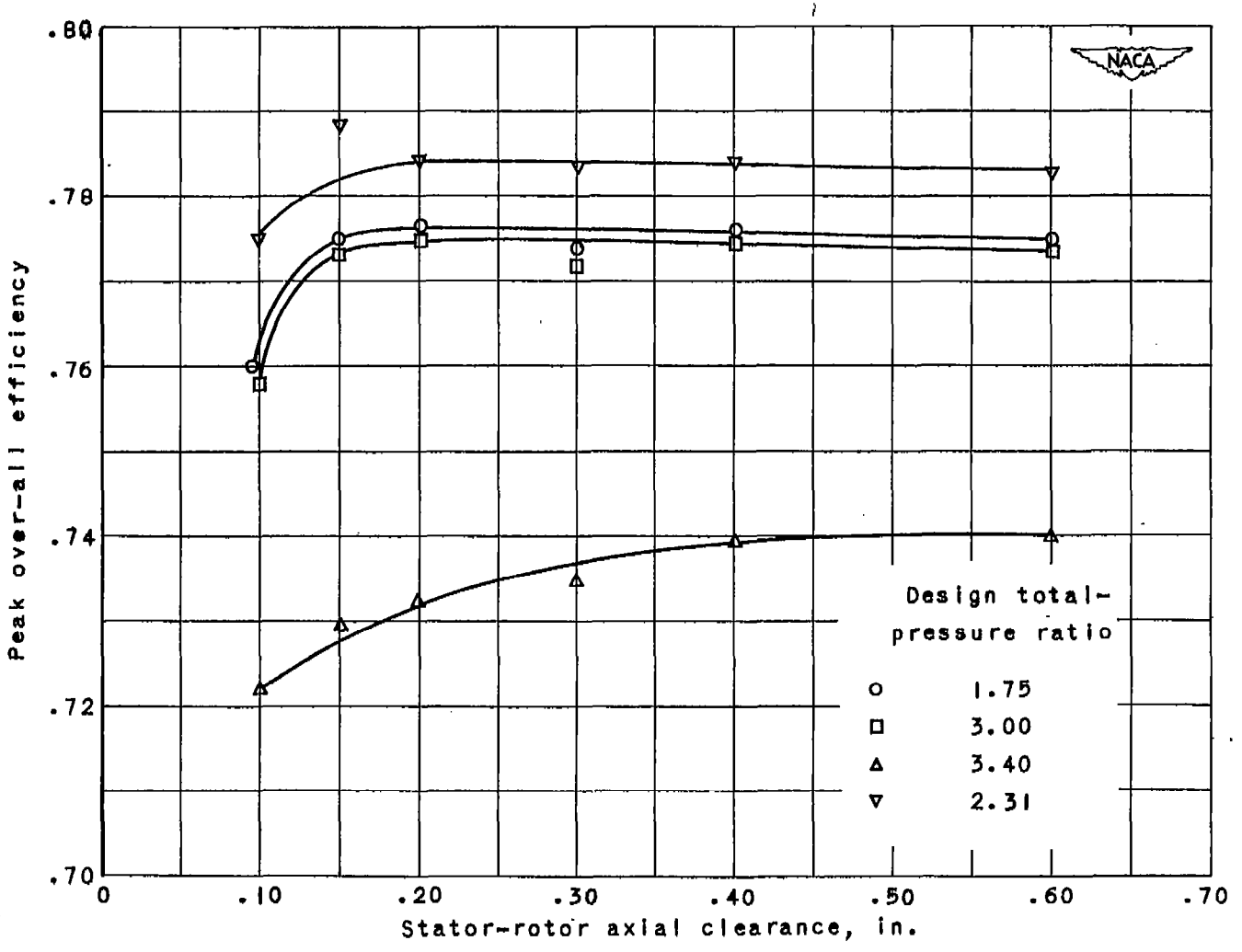

Figure 2. - Turbine peak efficiency plotted against axial clearance for model reaction turbine. (From unpublished data of Wright Aeronautical Corporation.)

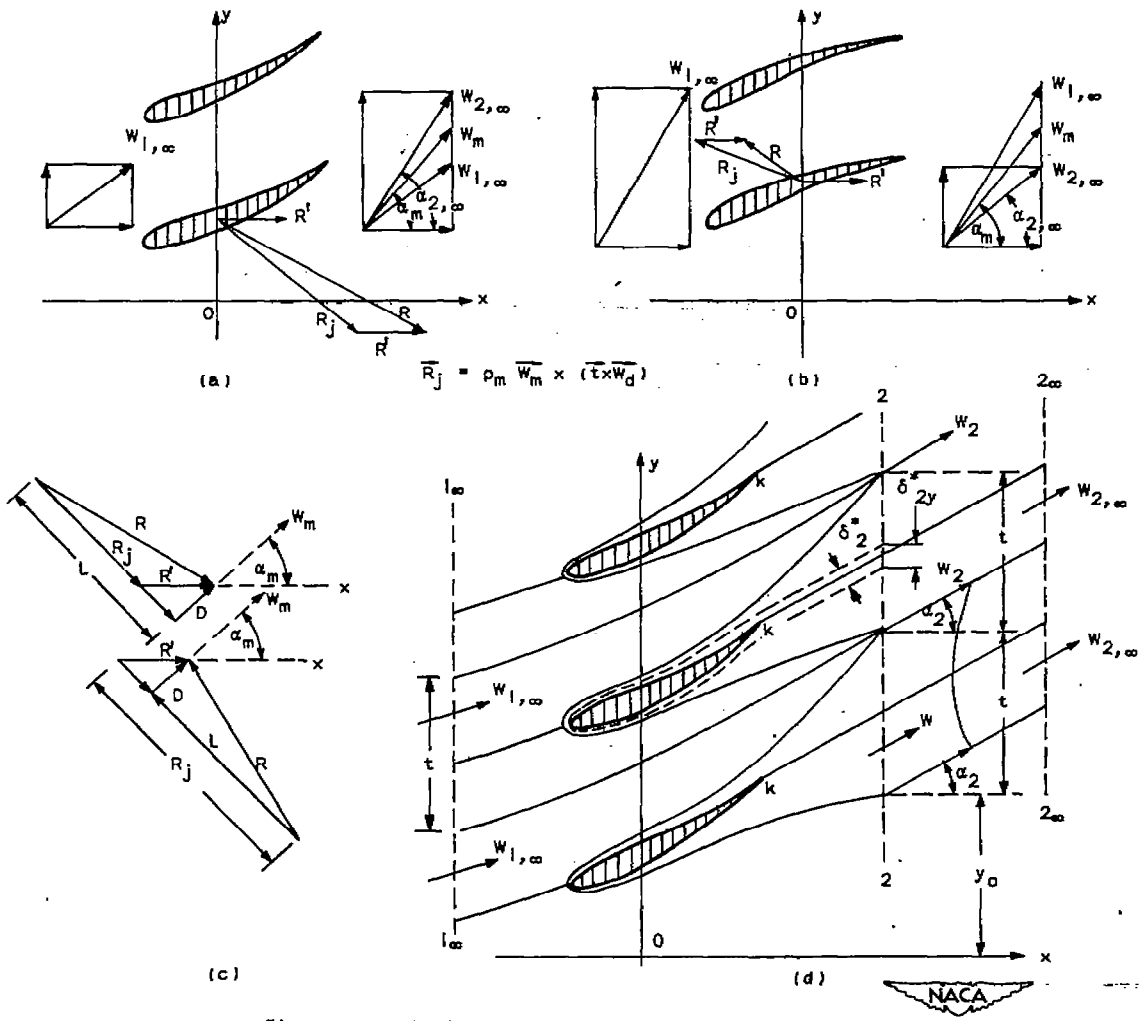

Figure 3. - Resistance of airfoil in cascade.

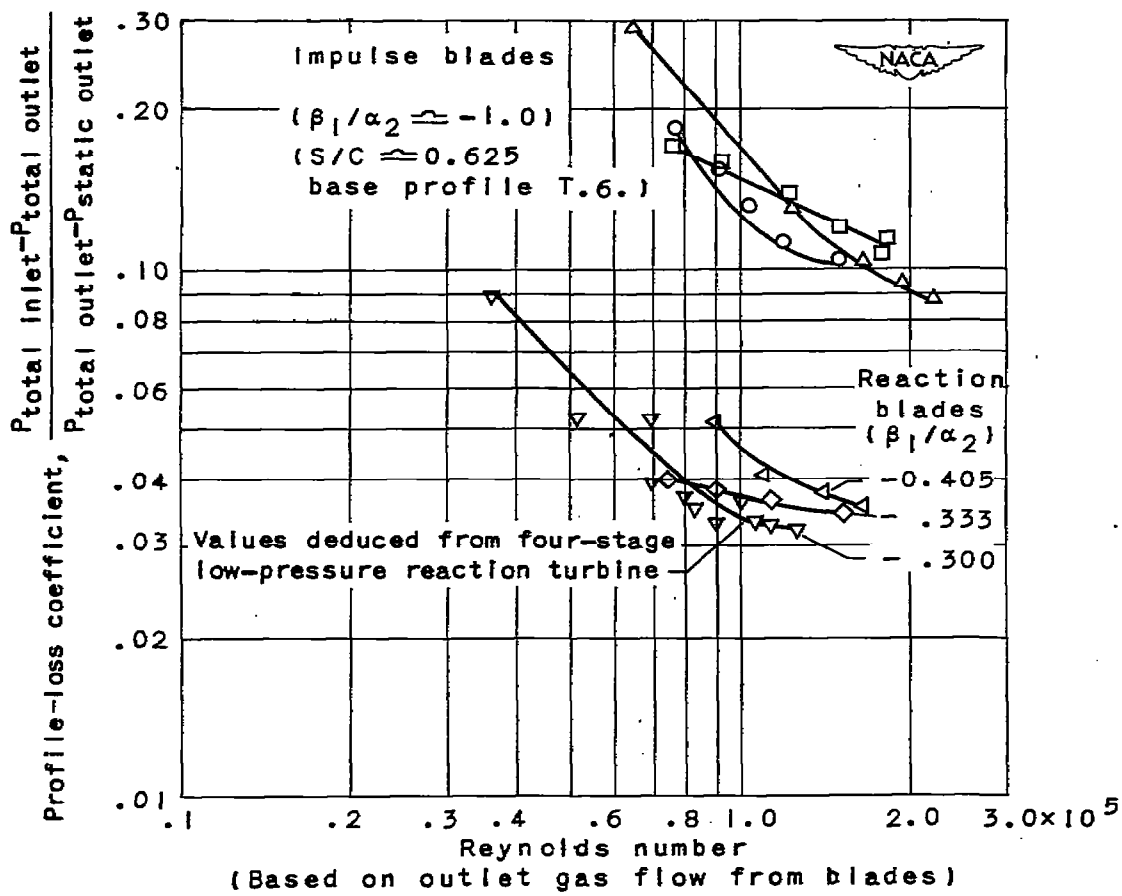

Figure 4. – Variation of profile loss with Reynolds number. (From reference 9.)

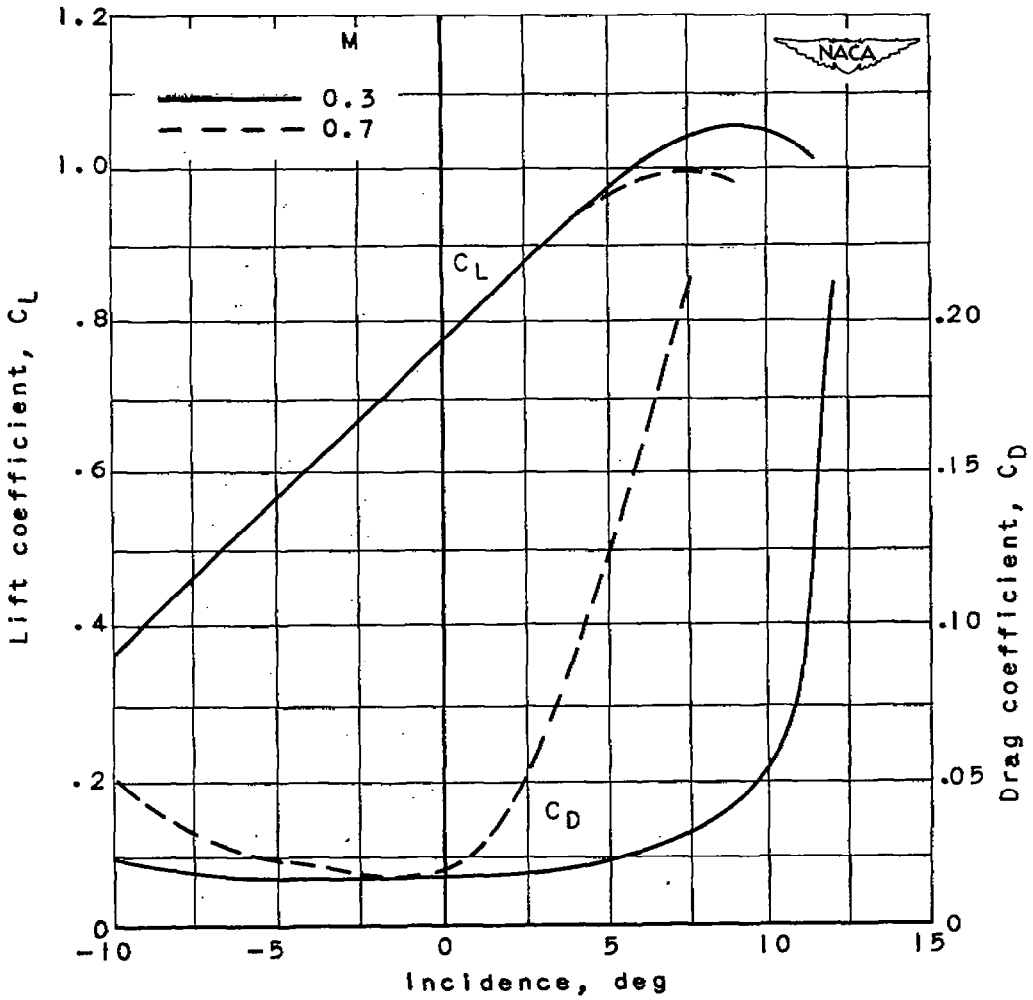

Figure 5. - Typical compressor cascade results.
(From reference 11.)

$\beta_1 = 55^\circ$ $\beta_2 = 30^\circ$
a/C = 0.4 S/C = 0.75
$\theta = 25^\circ$ t/C = 10 percent

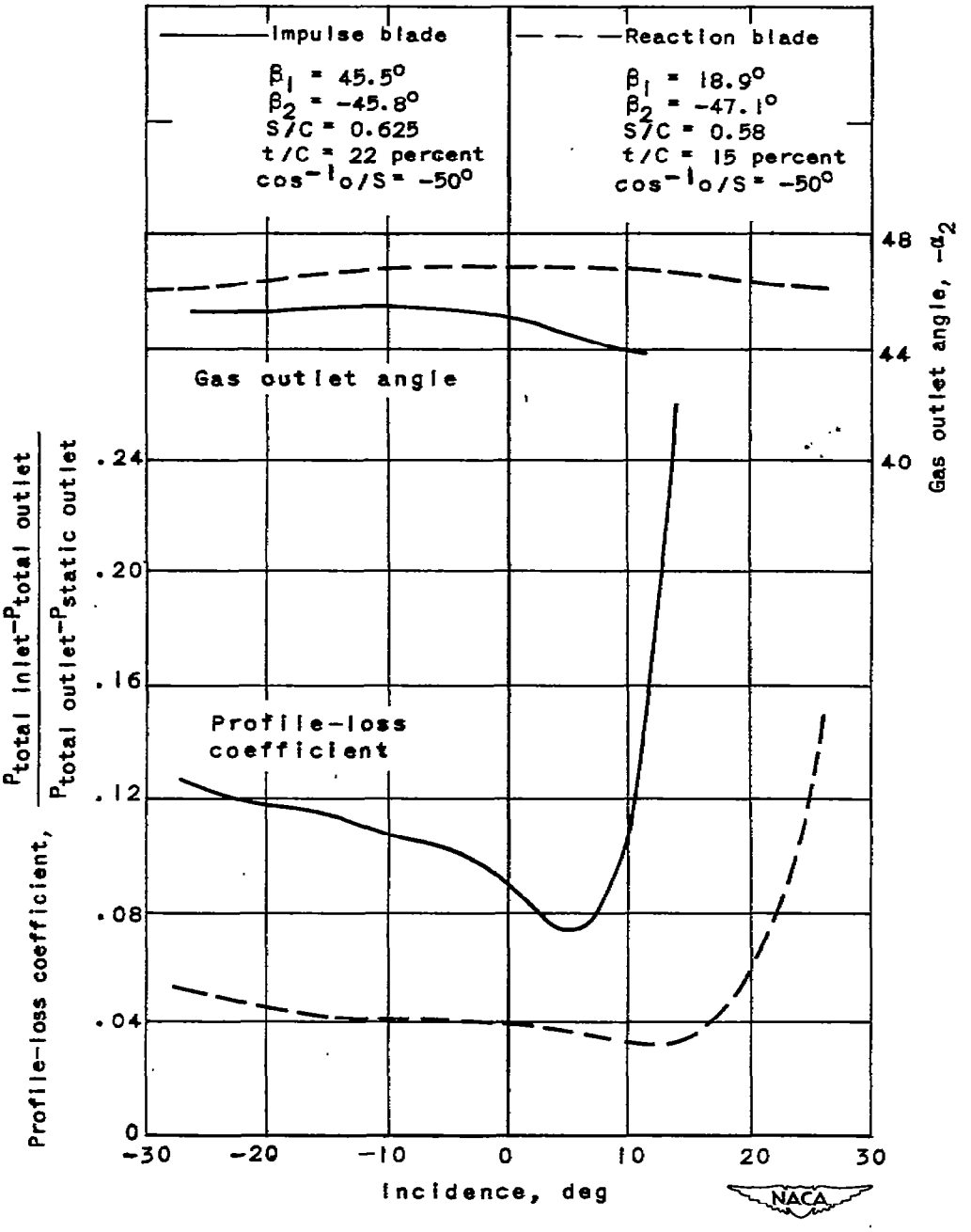

Figure 6. - Variation in profile loss with incidence for typical turbine blades. Base profile, T.6; a/C = 43 percent; Reynolds number $\approx 1.5 \times 10^5$; Mach number at outlet ≈ 0.5. (From reference 9.)

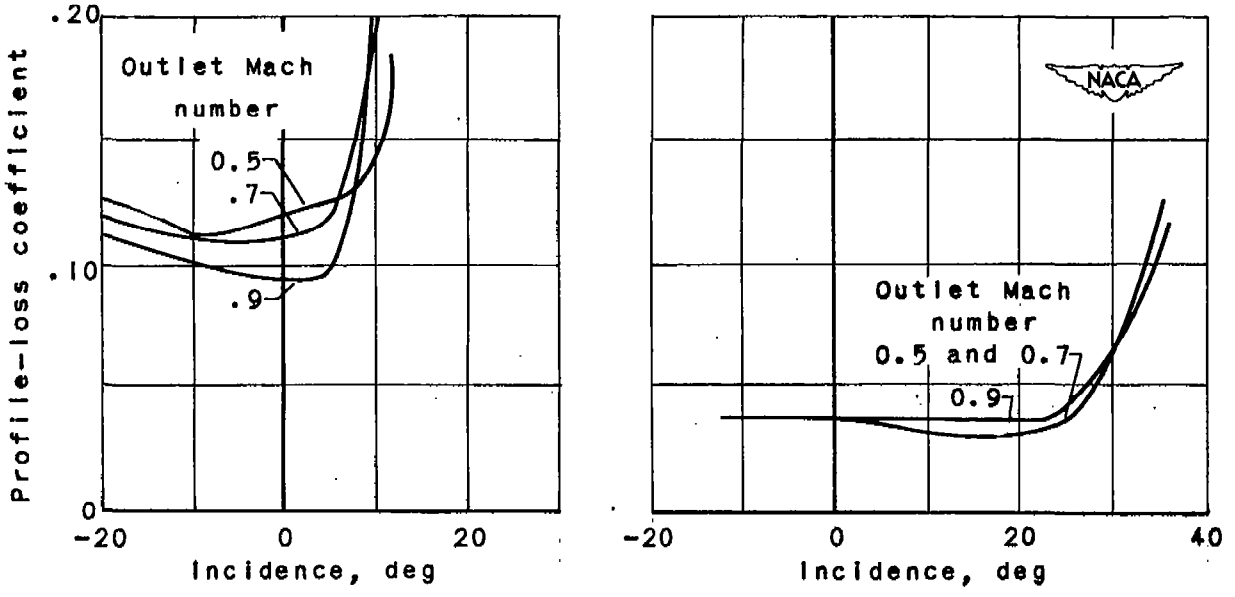

(a) Impulse blade.

$\cos^{-1} o/S = -60^{\circ}$

$\beta_1/\alpha_2 = -0.97$

S/C = 0.627

t/C = 31.3 percent

(b) Reaction blade.

$\cos^{-1} o/S = -60^{\circ}$

$\beta_1/\alpha_2 = -0.33$

S/C = 0.551

t/C = 18.1 percent

Figure 7. - Variation of blade loss with Mach number. (From reference 9.)

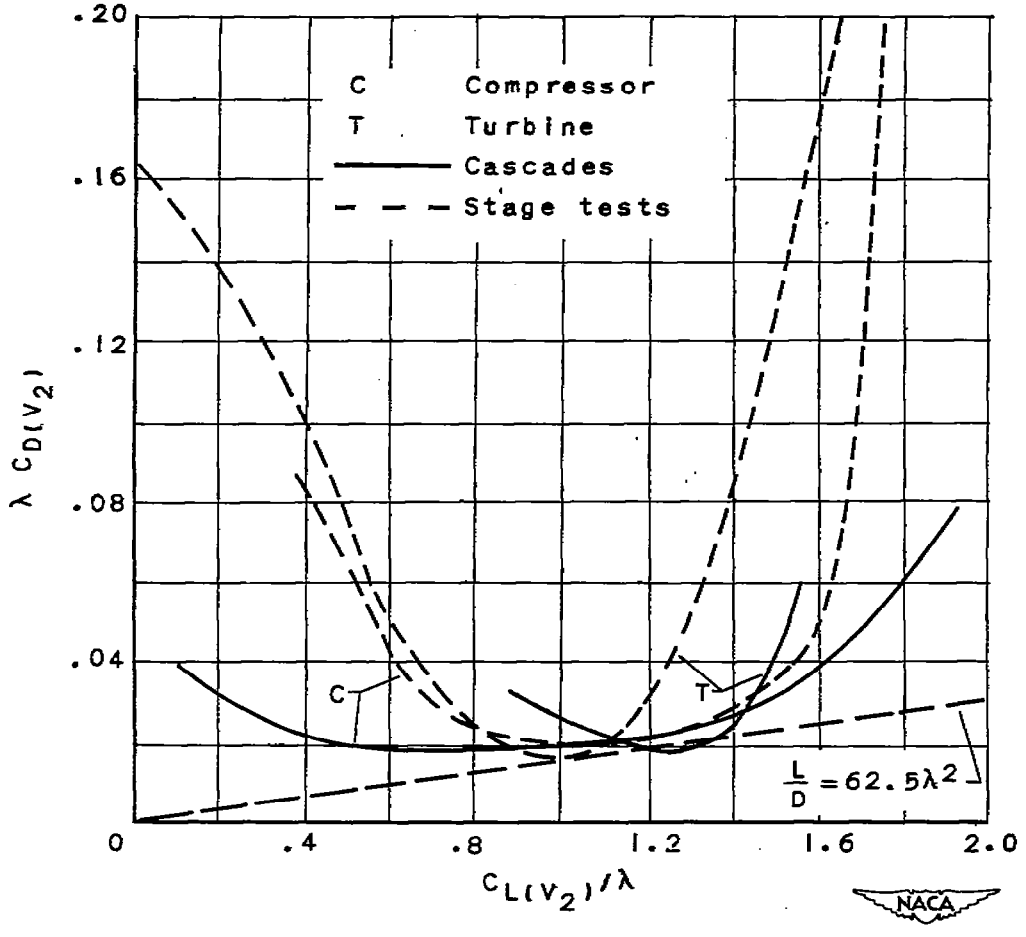

Figure 8. - Lift and drag coefficients based on outlet velocities. (From reference 11.)

$$\lambda = \frac{6(S/C) - 1}{5(S/C)} = \frac{6 - \sigma}{5}$$

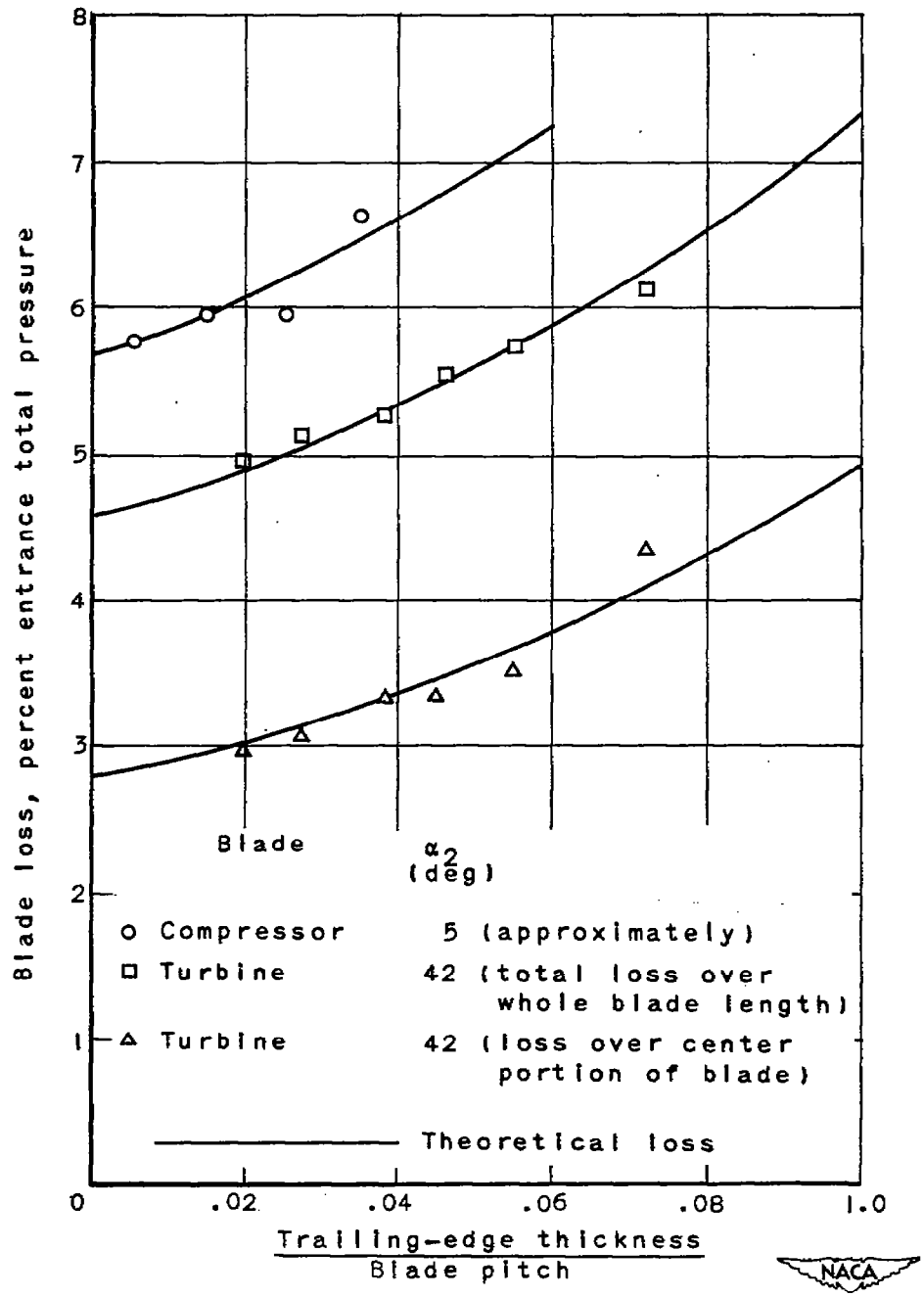

Figure 9. - Effect of trailing-edge thickness on blade-profile loss. (Reeman and Simonis.)

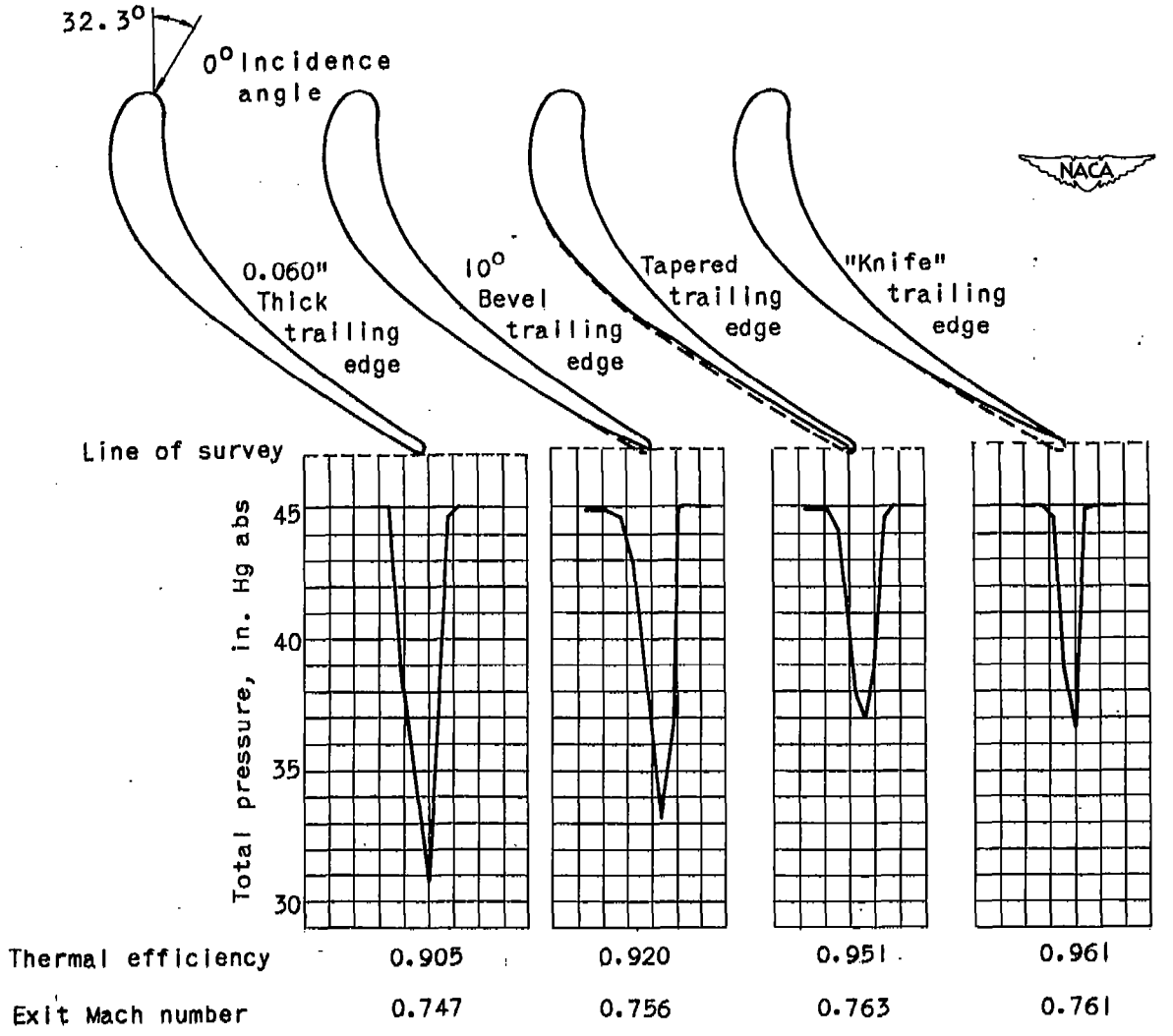

Figure 10. - Variation of wake profile and loss with different trailing-edge thickness and taper. (From unpublished data of Wright Aeronautical Corporation.)

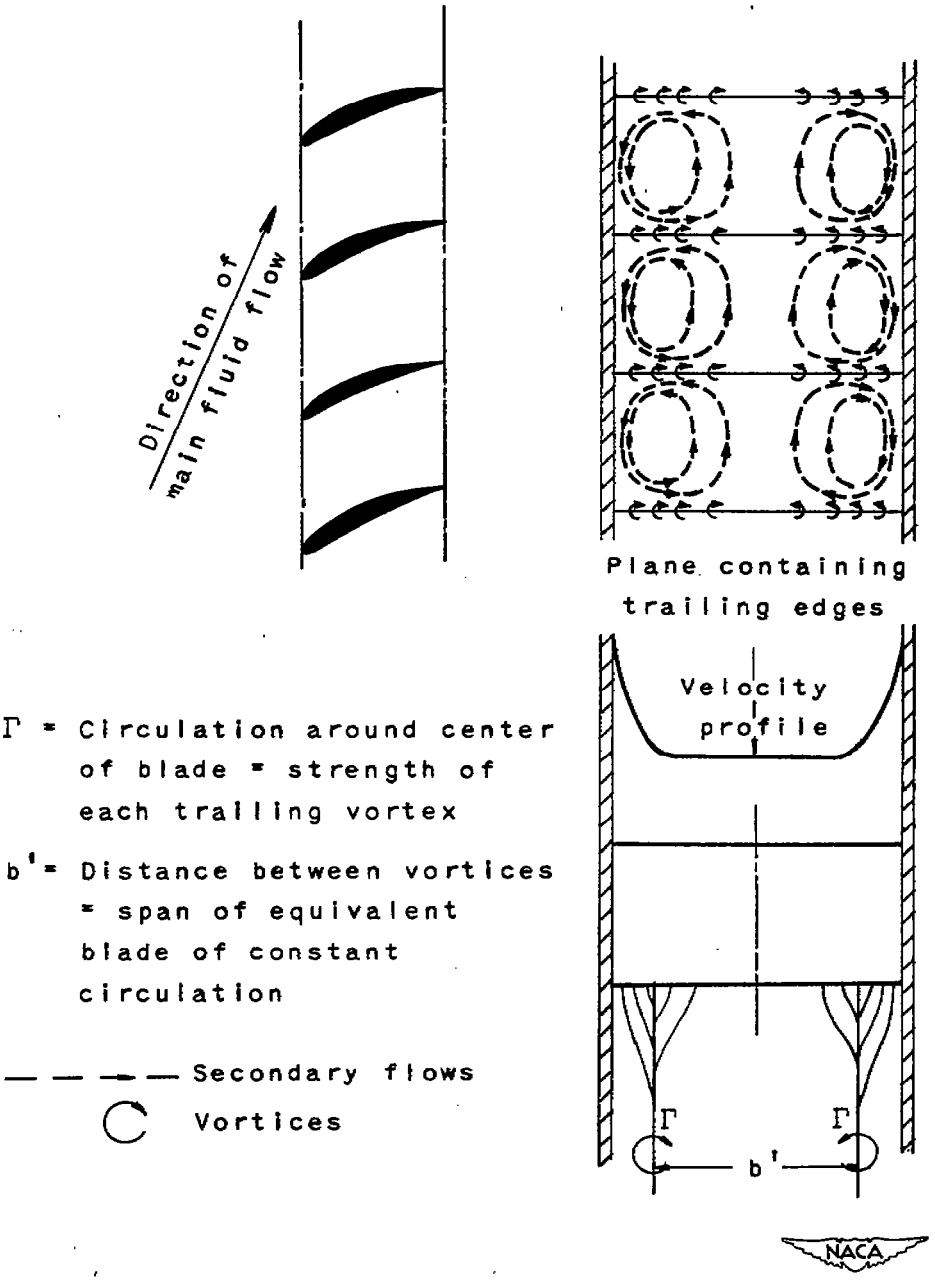

Figure 11. - Secondary flows in cascade.
(From reference 3.)

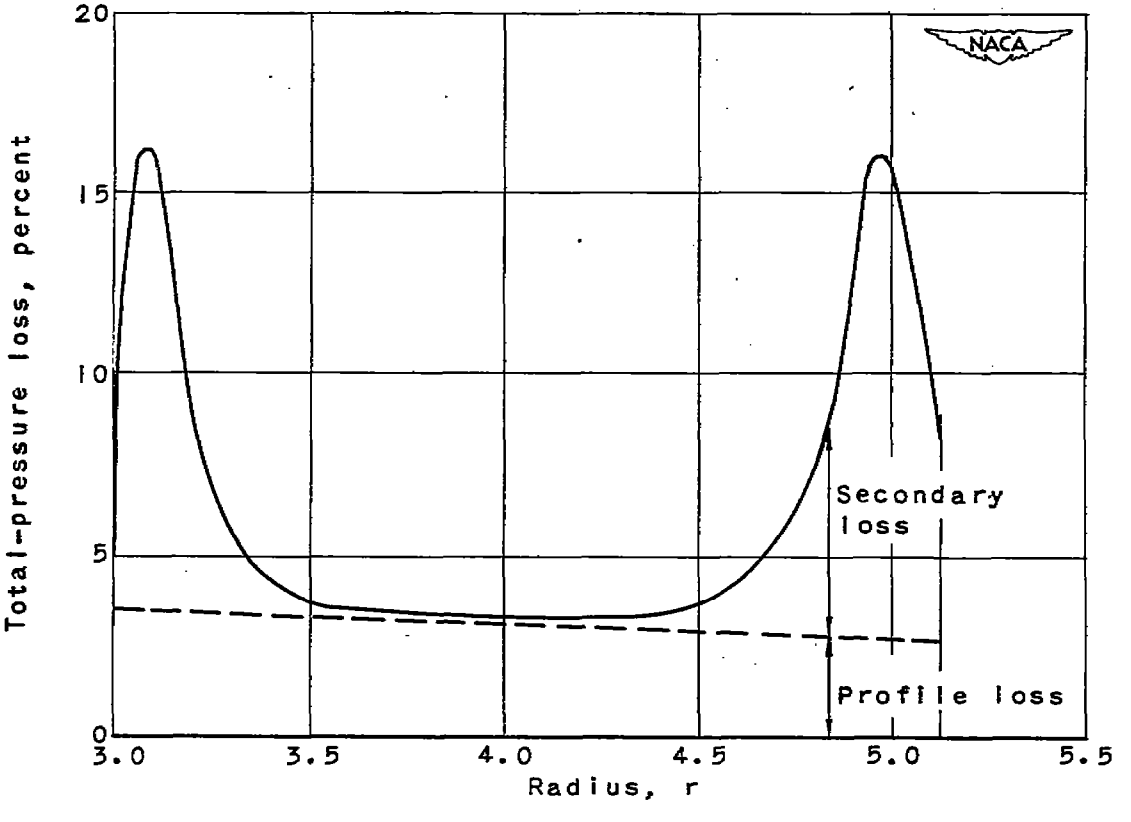

Figure 12. – Total-pressure loss due to secondary flow in an annulus. (From reference 3.)

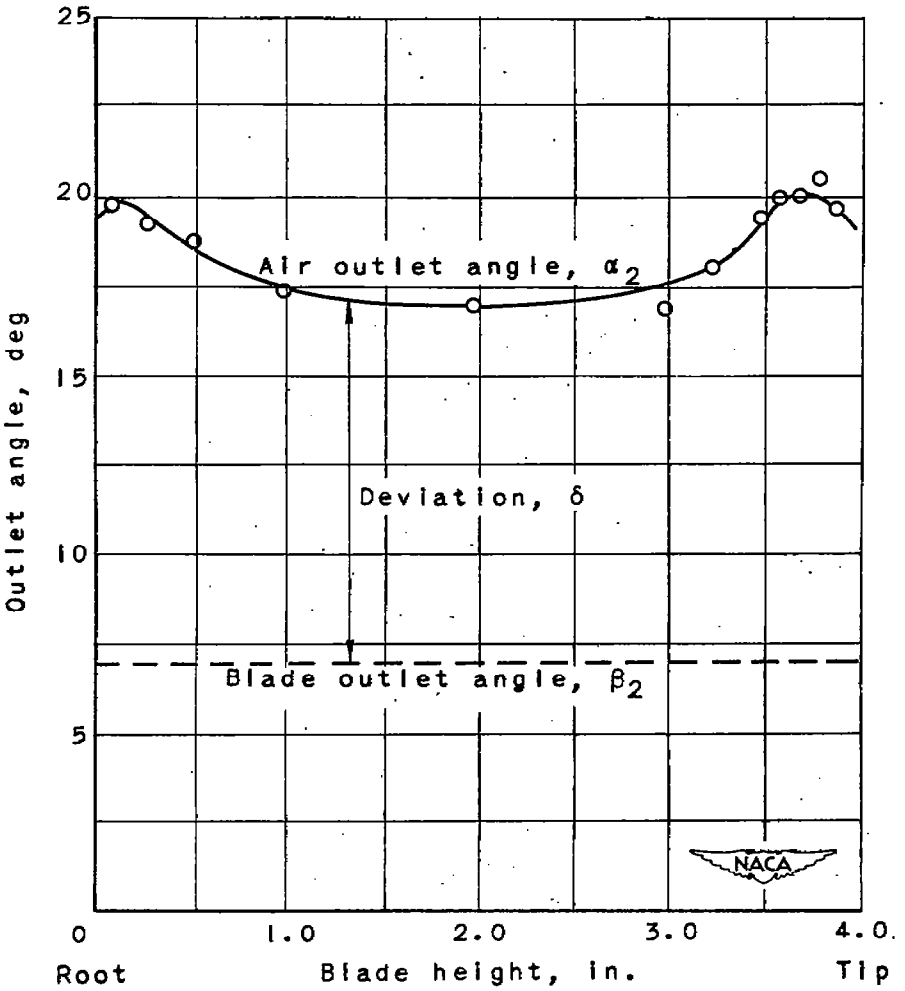

Figure 13. - Variation of outlet angle along blade height. Pitch/chord, 1.0. (From reference 3.)

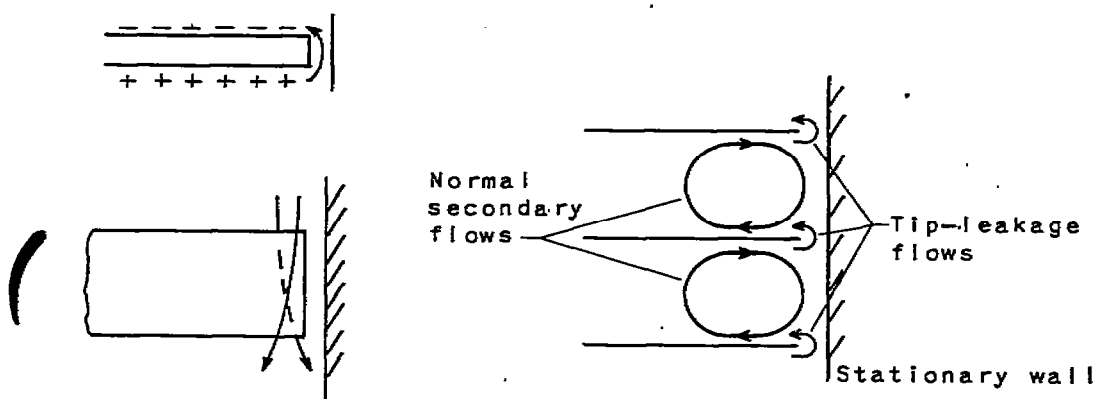

Figure 14. - Leakage flows due to tip clearance.

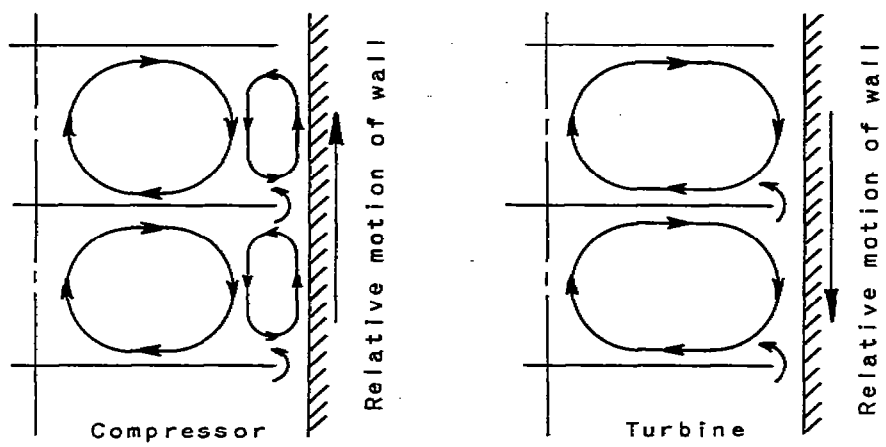

Motion of annulus wall aids tip leakage: entrained fluid sets up additional secondary flow.

Motion of annulus wall opposes tip leakage: fluid augments normal secondary flow.

Figure 15. - Secondary flows due to rotating annulus wall. (From reference 3.)

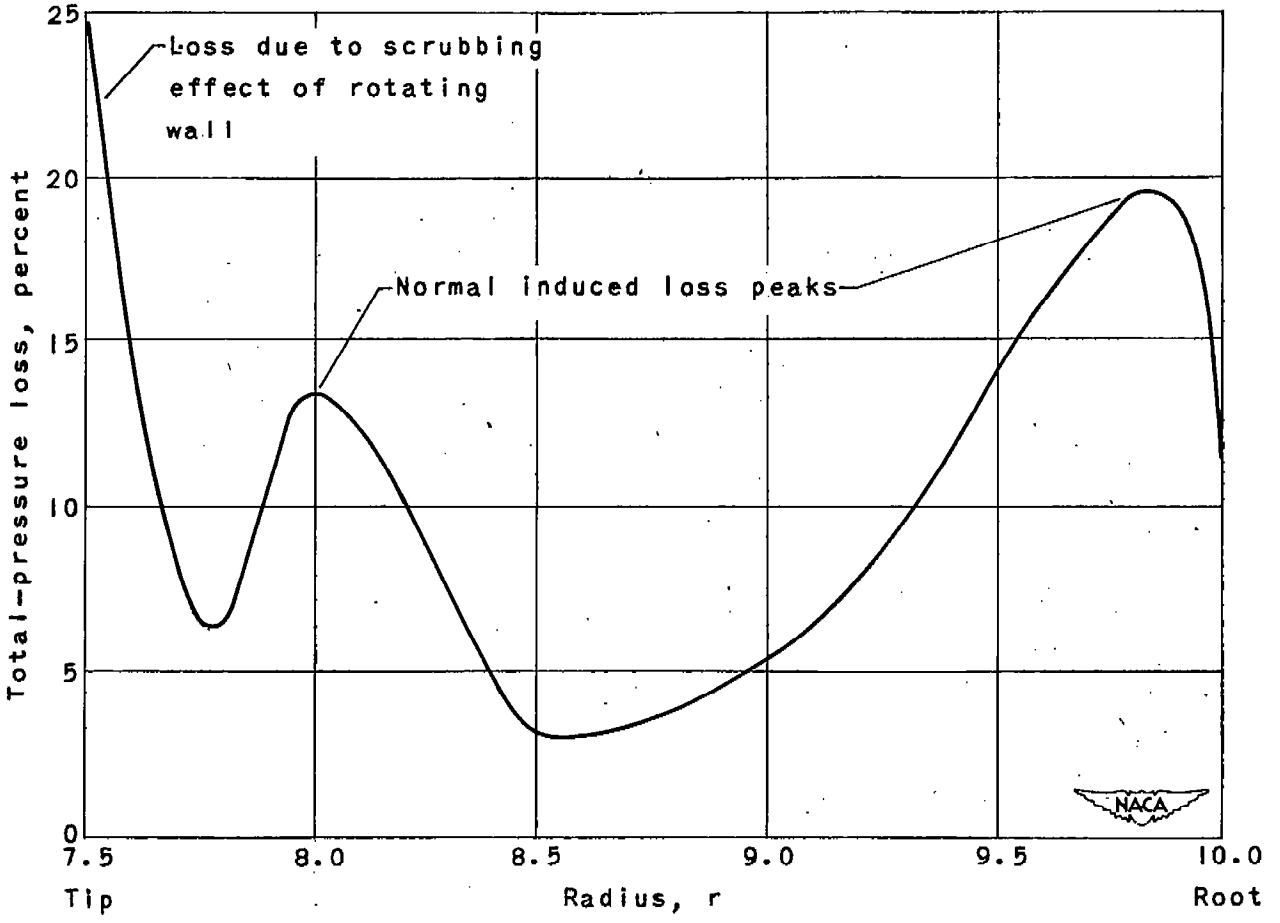

Figure 16. - Total-pressure losses due to secondary flow in compressor. (From reference 3.)

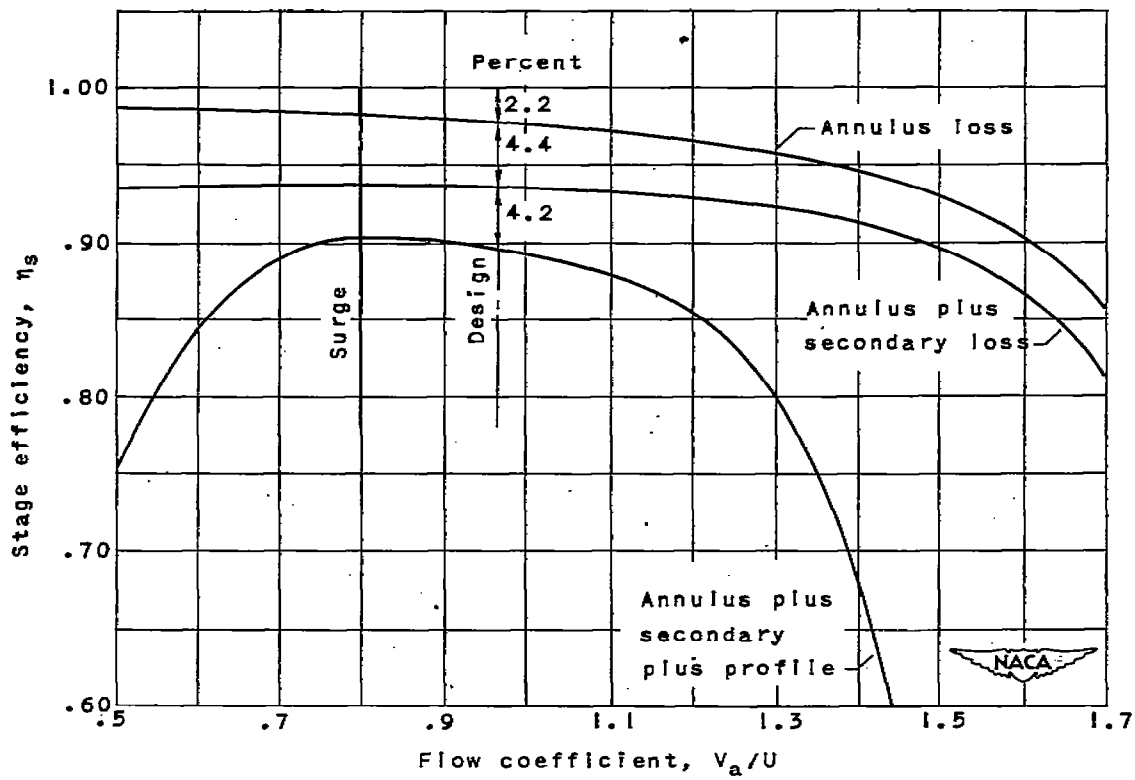

Figure 17. – Variation of losses with flow coefficients in a compressor. (From reference 3.)

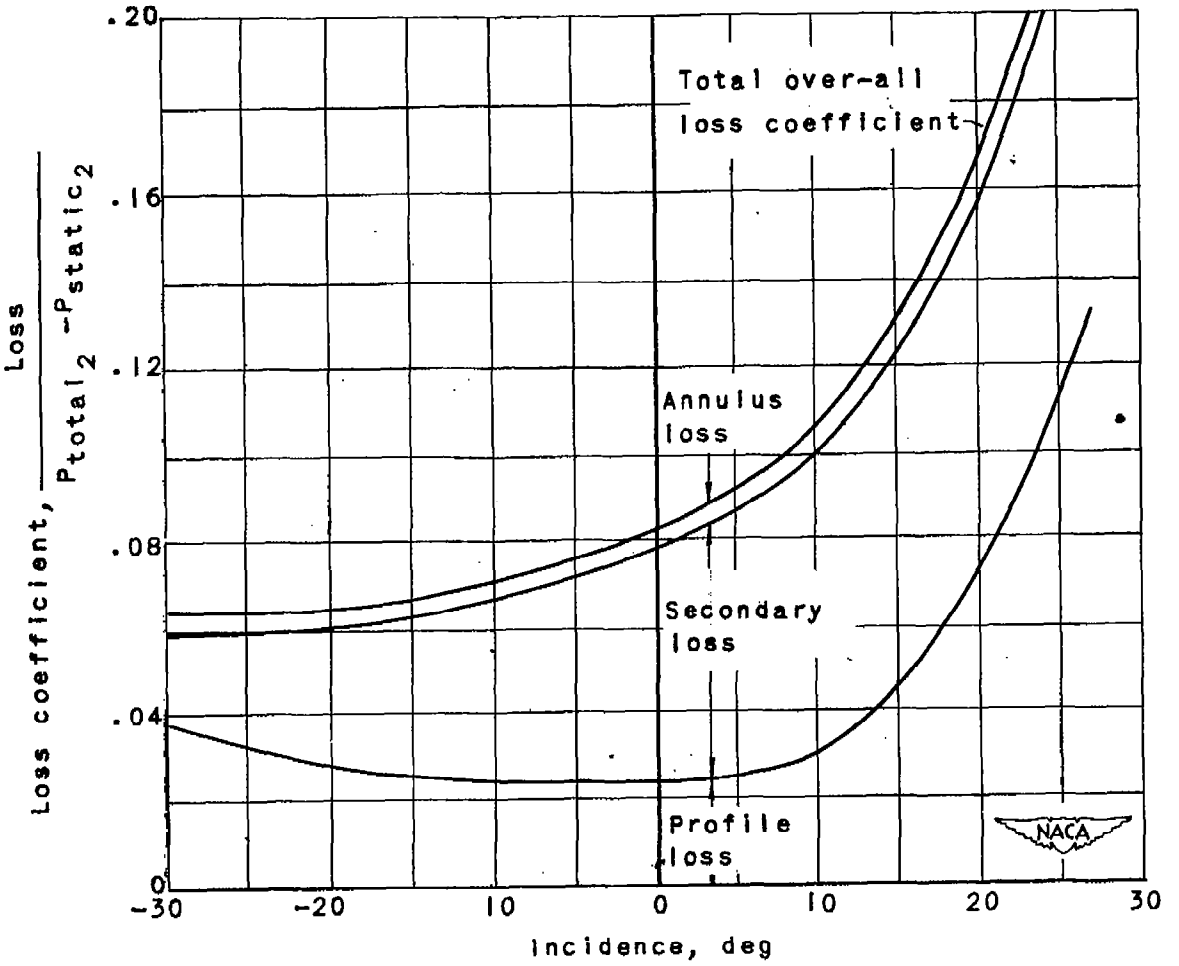

Figure 18. - Analysis of energy losses in flow through row of turbine blades. (From reference 9.)

NACA-Langley - 1-26-51 - 625